CHAPTER IV

EXPERIMENTAL RESULTS

4.1 Calibration of steel tube

Fig. 4 and 5 show the relationship between the temperature of an oven and the temperature of the clay in the steel tubes during heating. The results shows that the temperatures of the clay in the steel tubes were the same as the temperature of the oven after the heating period of 6 hours.

Figs. 6 and 7 present the relationship between the temperature of clay in the steel tubes and the time of heating. The temperatures of oven during heating are kept constant at each selected temperatures of 35°C, 40°C, 50°C and 60°C. These curves show that the period of time for temperatures of clay in the steel tubes to reach the temperature of the oven were varried with the temperature of the oven. With these four selected oven temperatures, the temperature of clay in the steel tubes had to have a maximum period of 6 hours to reach the temperature of the oven at 60°C. This period of time is shorter than the selected heating period of 8 hours in the test.

4.2 Consolidated-undrained strength

The values of the maximum and minimum effective stresses of the heated and unheated soil were collected and presented as shown in Table 2. The results show that the soil samples which have natural water content ranging from 82.82 % to 63.44 % (samples B-1 to B-4) decrease their maximum effective stresses with the increasing of the heating temperatures. The maximum effective stresses are shown to be increased with the increasing of heating temperatures when natural water content of the soil samples are in the range of 48.63 % to 28.56 % (samples B-5 to B-6).

Figs. 8 to 11 illustrate the examples of plotting the Mohr's circles of effective stresses and their tangent lines for the sample B-1, which is unheated and heated at 40°C, 50°C and 60°C.

Figs. 12 to 17 present the comparison of the tangent lines of the Mohr's circles of the unheated and heated samples which were obtained from various depth. The comparisons show that when the heating temperature increase the angles of internal friction and the cohesions of the soil samples which have the natural water content ranging from 82.82 % to 63.44 % decrease. Moreover, the soil samples which have the natural water content ranging from 48.63 % to 28.56 % give the slightly increasing of both angles of internal friction and cohesions.

4.3 Consolidation

Figs. 18 to 23 show the comparison of the e-log p curves of unheated and heated samples which were selected from various depth. The curves show that at the same consolidation pressure, the higher void ratio for all samples are introduced as a result of increasing temperature.

Figs. 24 to 29 show the ploted of the coefficient of consolidation at 90 % consolidation which were tested at different heated temperatures. The curves indicate that at the same consolidation pressure, the higher temperature of heating gives the lower coefficient of consolidation.

TABLE 2 MAXIMUM AND MINIMUM EFFECTIVE STRESSES, ANGLE OF INTERNAL FRICTION AND COHESIONS OF THE BANGKOK CLAY SAMPLES TESTED AT DIFFERENT TEMPERATURES.

SAMPLE & DEPTH		NAT. WATER CONTENT (%)	TEMP. OF HEATING (^oC)	CELL PRESS. (KSC)	σ_1 MAX. (KSC)	σ_3 MAX. AT σ_1 MAX. (KSC)	ANGLE OF INTERNAL FRICTION (^{o})	COHESION (KSC)
SAMPLE NO.	DEPTH FROM-TO (M.) (M.)							
B - 1	2.75-3.30	82.82	UNHEATED	3.5	5.682	3.288	11.0^o	0.30
				4.0	6.302	3.720		
				4.5	7.159	4.320		
			40	3.5	5.452	3.337	10.0	0.28
				4.0	6.074	3.882		
				4.5	6.944	4.382		
			50	3.5	5.017	3.337	9.5	0.25
				4.0	5.937	3.857		
				4.5	6.753	4.362		
			60	3.5	4.878	3.143	8.5	0.23
				4.0	5.602	3.700		
				4.5	6.469	4.307		
B - 2	6.75-7.30	80.65	UNHEATED	3.5	5.150	3.208	8.0	0.48
				4.0	6.052	3.751		
				4.5	6.843	4.327		
			40	3.5	5.021	3.182	7.5	0.45
				4.0	5.951	3.754		
				4.5	6.674	4.350		
			50	3.5	4.910	3.262	7.5	0.35
				4.0	5.824	3.777		
				4.5	6.601	4.335		
			60	3.5	4.855	3.137	7.0	0.35
				4.0	5.718	3.738		
				4.5	6.212	4.290		
B - 3	8.75-9.30	73.89	UNHEATED	3.5	5.131	3.222	9.5	0.43
				4.0	6.342	3.891		
				4.5	7.111	4.414		
			40	3.5	5.125	3.183	8.5	0.40
				4.0	6.051	3.758		
				4.5	7.015	4.333		
			50	3.5	5.016	3.155	8.2	0.40
				4.0	6.017	3.790		
				4.5	6.964	4.431		
			60	3.5	4.942	3.120	8.0	0.35
				4.0	5.926	3.721		
				4.5	6.793	4.312		

SAMPLE & DEPTH		NAT. WATER CONTENT (%)	TEMP. OF HEATING (^oC)	CELL PRESS. (KSC)	σ_1 MAX. (KSC)	σ_3 MAX. AT σ_1 MAX. (KSC)	ANGLE OF INTERNAL FRICTION (^{o})	COHESION (KSC)
SAMPLE NO.	DEPTH FROM-TO (M.) (M.)							
B - 4	10.75-11.30	63.44	UNHEATED	3.5	5.739	3.095	12.5	0.38
				4.0	6.525	3.680		
				4.5	7.624	4.260		
			40	3.5	5.588	3.128	12.0	0.33
				4.0	6.389	3.725		
				4.5	7.482	4.322		
			50	3.5	5.445	3.277	11.5	0.30
				4.0	6.293	3.780		
				4.5	7.350	4.321		
			60	3.5	4.906	3.195	11.0	0.30
				4.0	6.095	3.850		
				4.5	7.152	4.504		
B - 5	12.75-13.30	48.63	UNHEATED	3.5	6.012	3.261	10.5	0.50
				4.0	6.851	3.797		
				4.5	8.014	4.305		
			40	3.5	6.127	3.258	12.0	0.55
				4.0	7.013	3.725		
				4.5	8.152	4.430		
			50	3.5	6.288	3.233	12.5	0.60
				4.0	7.222	3.709		
				4.5	8.240	4.340		
			60	3.5	6.779	3.371	13.0	0.63
				4.0	7.418	3.752		
				4.5	8.502	4.414		
B - 6	14.75 15.30	28.56	UNHEATED	3.5	6.290	3.318	11.8	0.48
				4.0	7.102	3.828		
				4.5	8.109	4.445		
			40	3.5	6.398	3.318	12.0	0.55
				4.0	7.189	3.782		
				4.5	8.149	4.345		
			50	3.5	6.598	3.251	13.0	0.55
				4.0	7.355	3.832		
				4.5	8.532	4.457		
			60	3.5	6.657	3.302	13.5	0.60
				4.0	7.500	3.854		
				4.5	8.452	4.459		

FIG. 4 RELATIONSHIP BETWEEN TEMPERATURE OF OVEN AND TEMPERATURE OF CLAY IN STEEL TUBE DURING HEATING

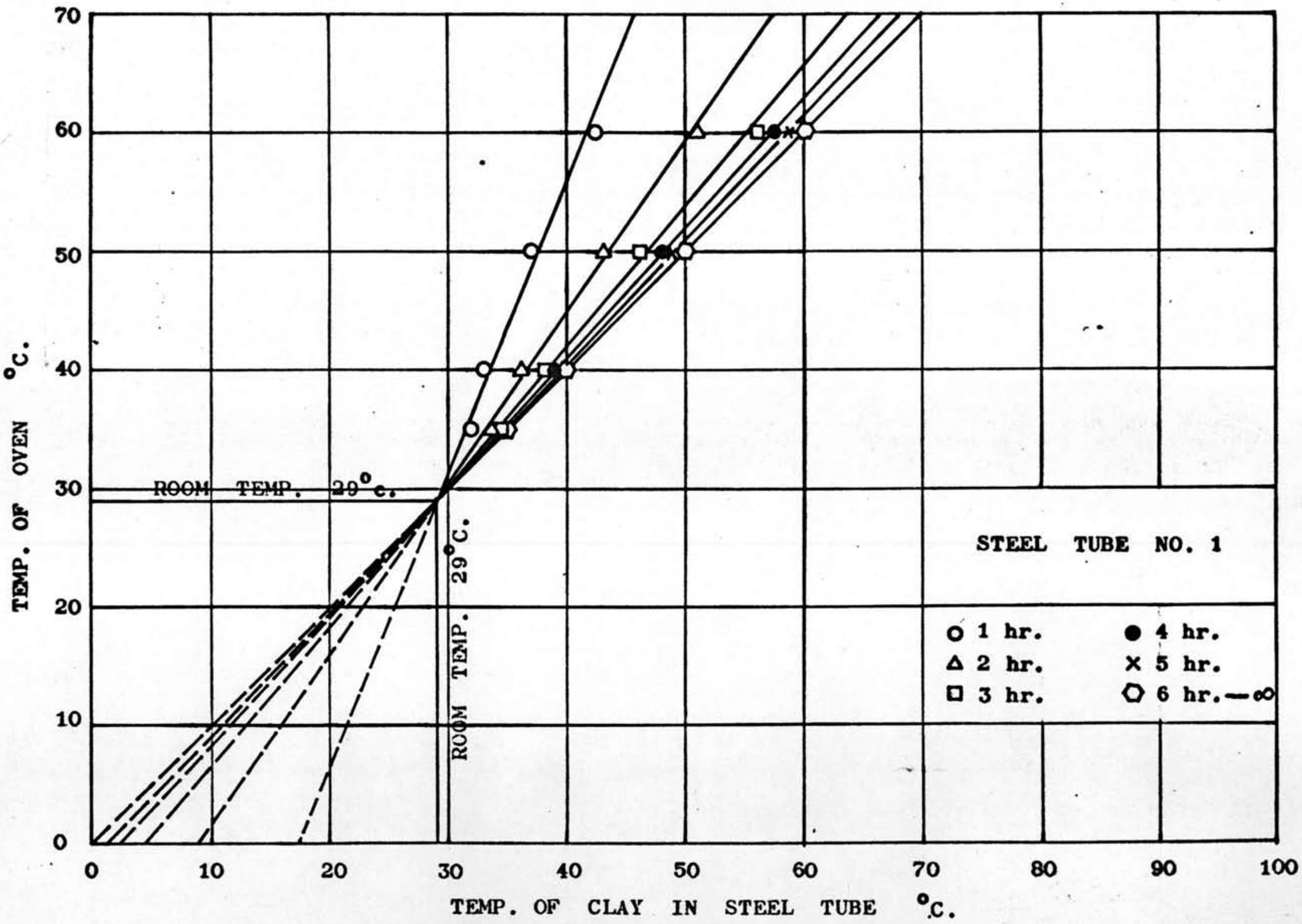

FIG. 5 RELATIONSHIP BETWEEN TEMPERATURE OF OVEN AND TEMPERATURE OF CLAY IN STEEL TUBE DURING HEATING

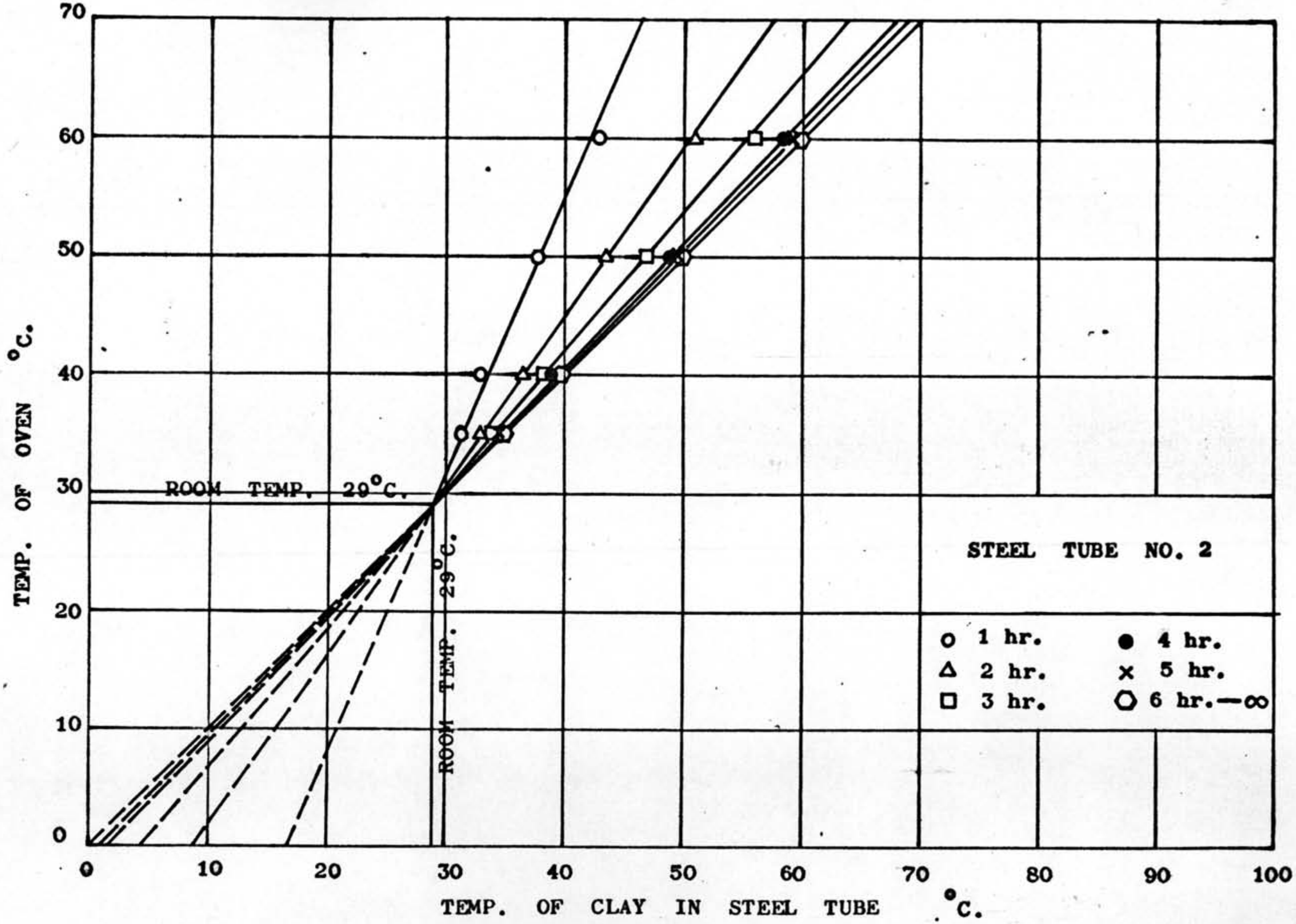

FIG. 6 RELATIONSHIP BETWEEN TEMPERATURE OF CLAY IN TUBE AND TIME OF HEATING, TEMPERATURE OF OVEN 35°C, 40°C, 50°C AND 60°C.
STEEL TUBE NO. 1

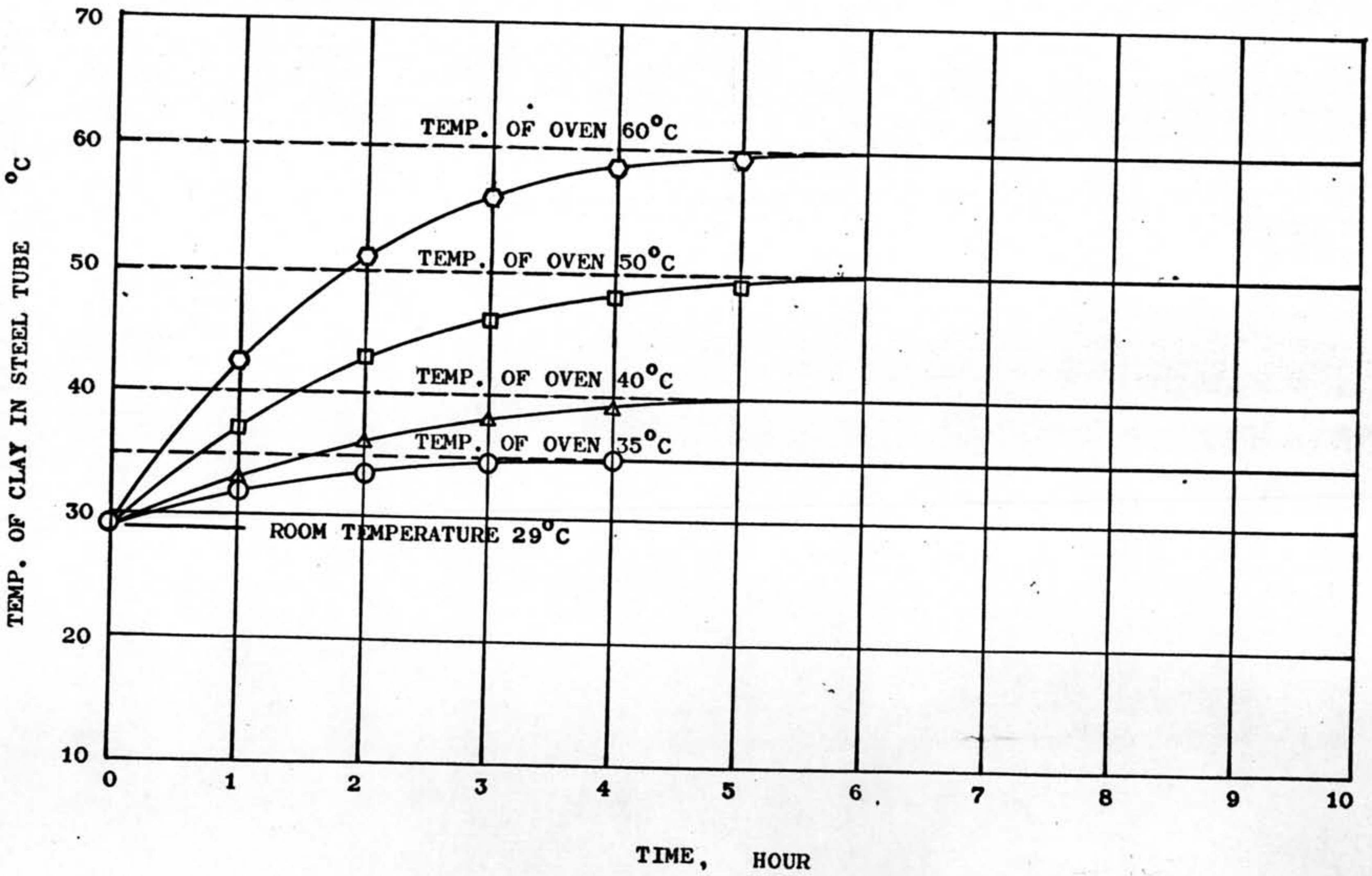

FIG. 7 RELATIONSHIP BETWEEN TEMPERATURE OF CLAY IN TUBE AND TIME OF HEATING, TEMPERATURE OF OVEN 35°C, 40°C, 50°C AND 60°C. STEEL TUBE NO. 2

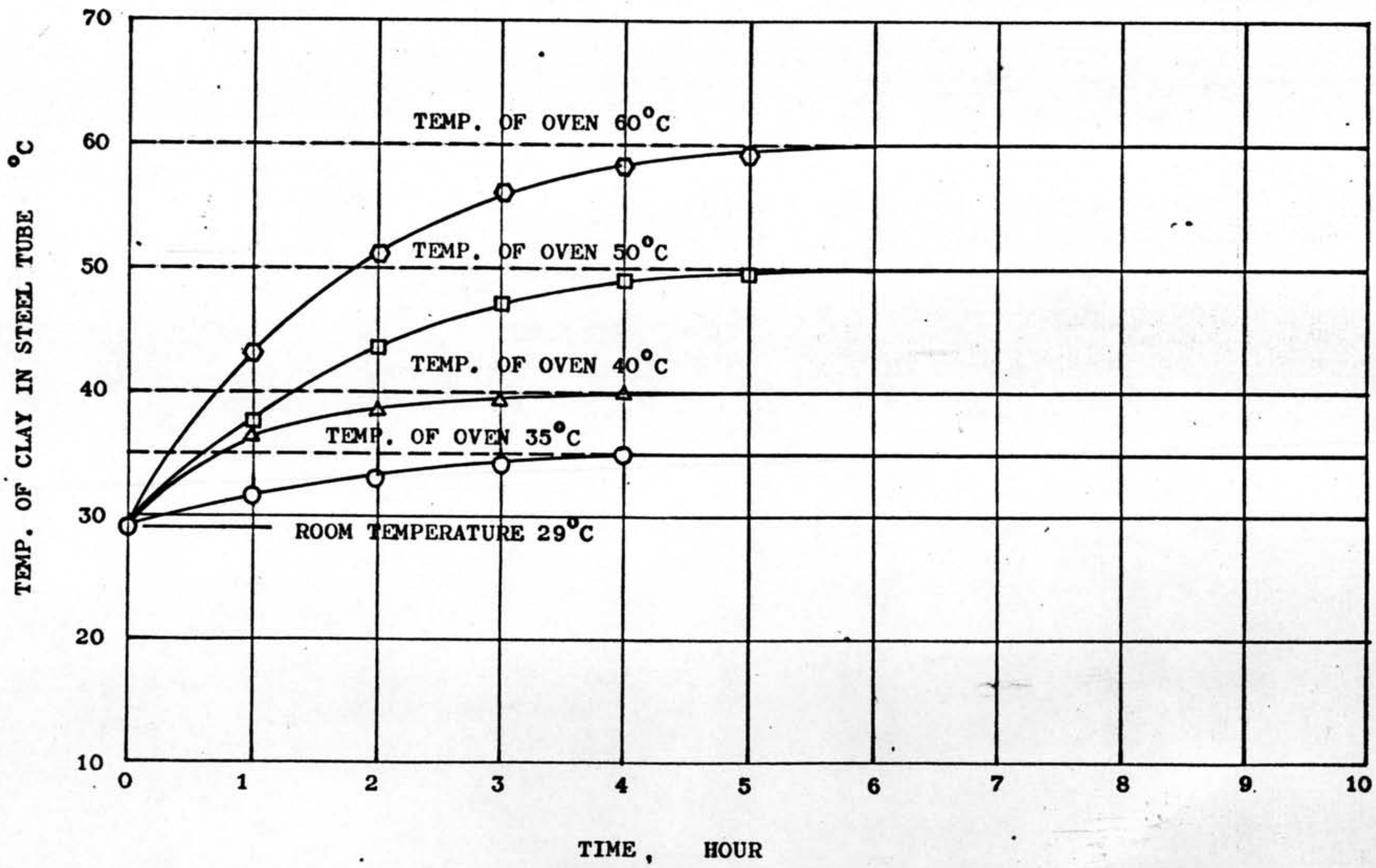

FIG. 8 MOHR'S CIRCLE OF CONSOLIDATED-UNDRAINED STRESSES FOR SAMPLE NO. B-1
UNHEATED SAMPLE

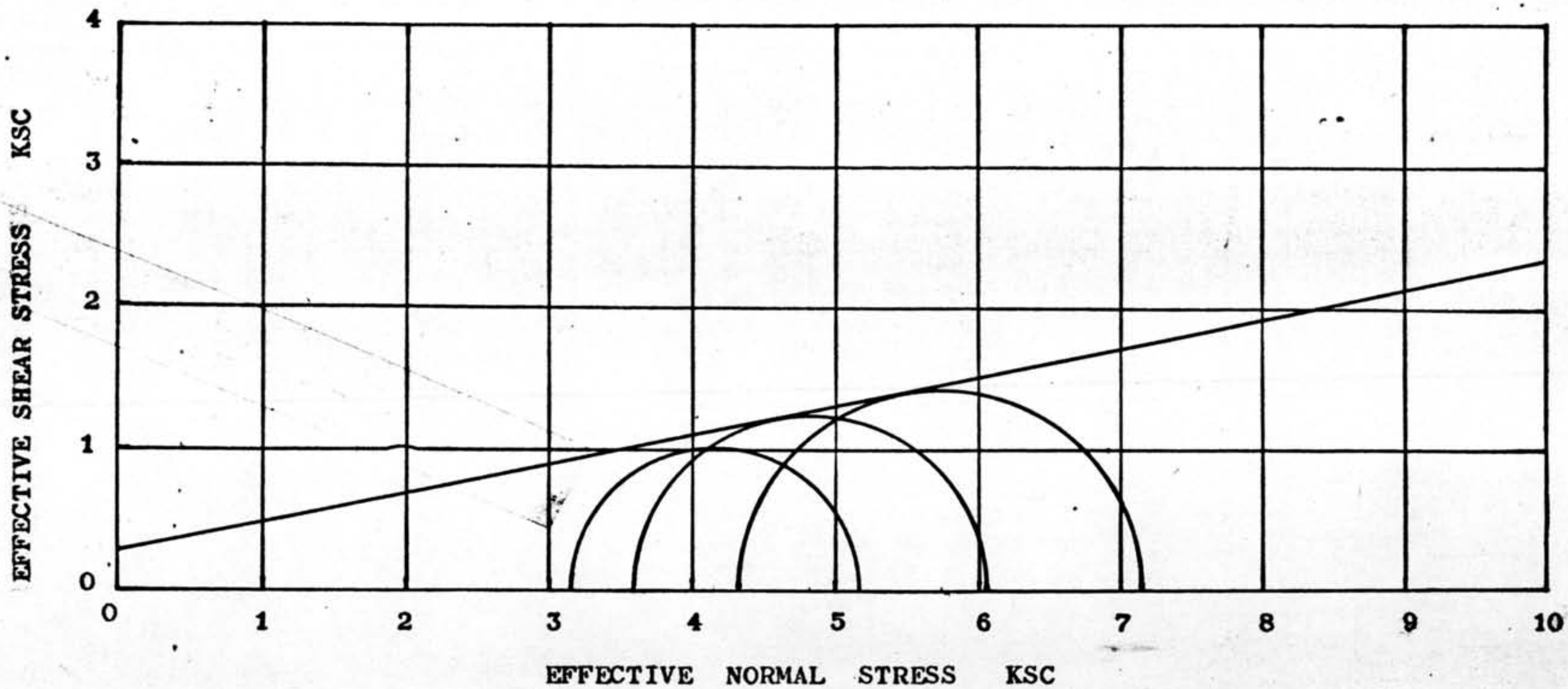

FIG. 9 MOHR'S CIRCLE OF CONSOLIDATED-UNDRAINED STRESSES FOR SAMPLE NO. B-1
HEATED SAMPLE (40°C)

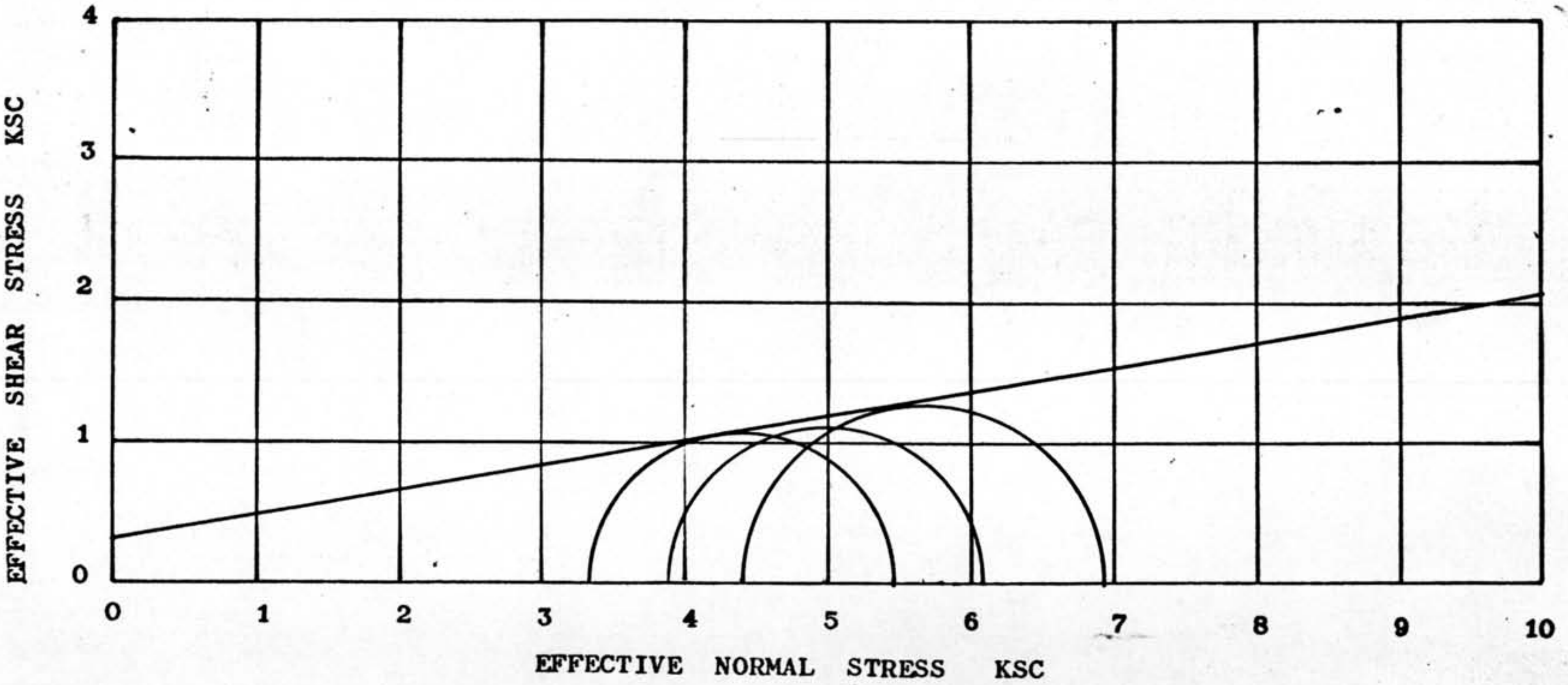

FIG. 10 MOHR'S CIRCLE OF CONSOLIDATED-UNDRAINED STRESS FOR SAMPLE NO. B-1 HEATED SAMPLE (50°C)

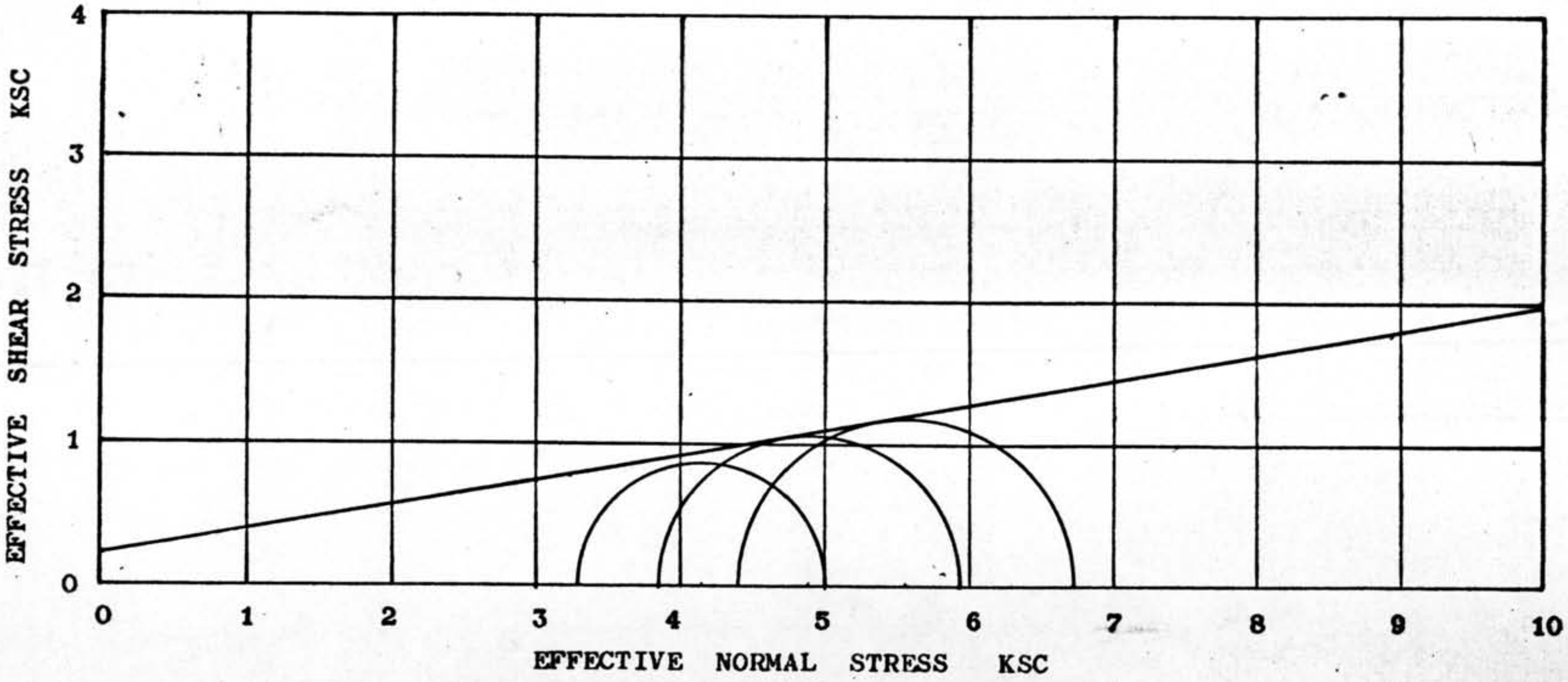

FIG. 11 MOHR'S CIRCLE OF CONSOLIDATED-UNDRAINED STRESS FOR SAMPLE NO. B-1
HEATED SAMPLE (60°C)

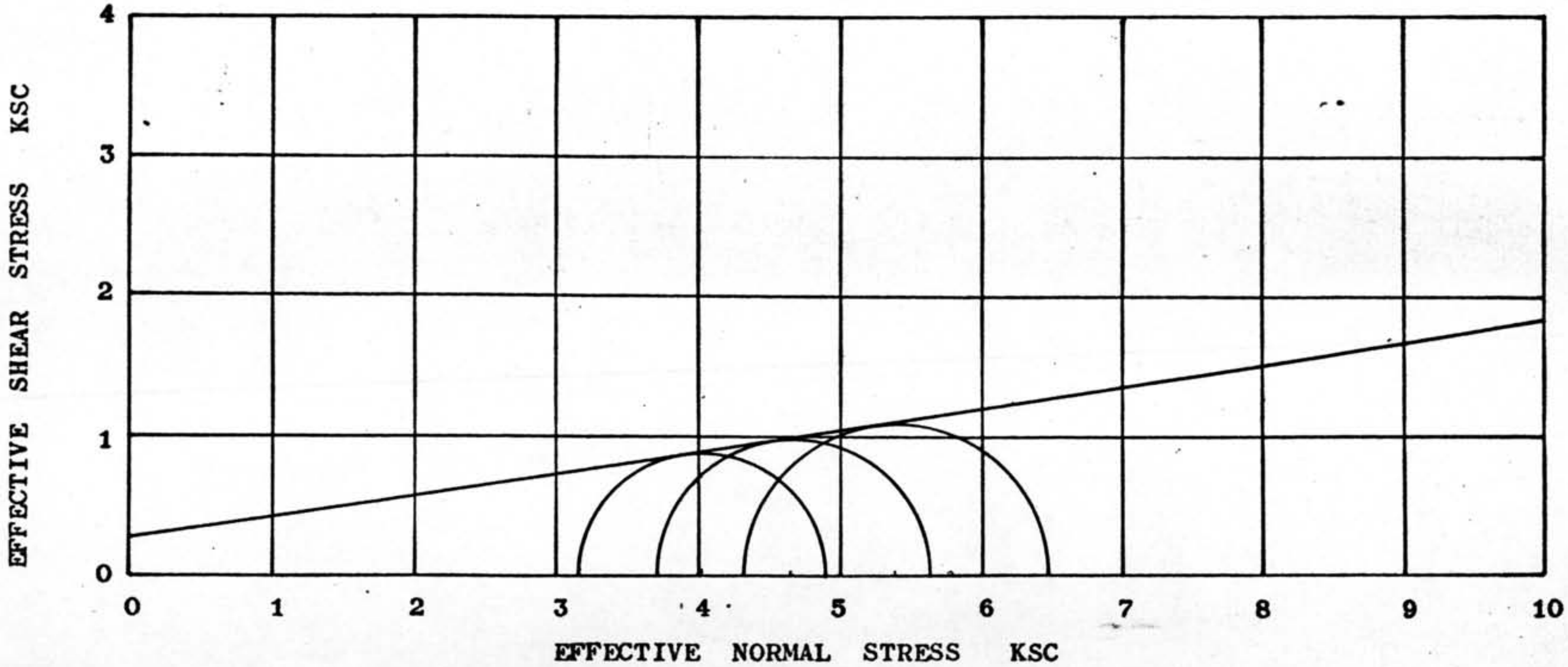

FIG. 12 COMPARISON OF TANGENT LINES OF MOHR'S CIRCLES, UNHEATED, HEATED AT 40°C, 50°C, AND 60°C SAMPLES.
SAMPLE NO. B-1

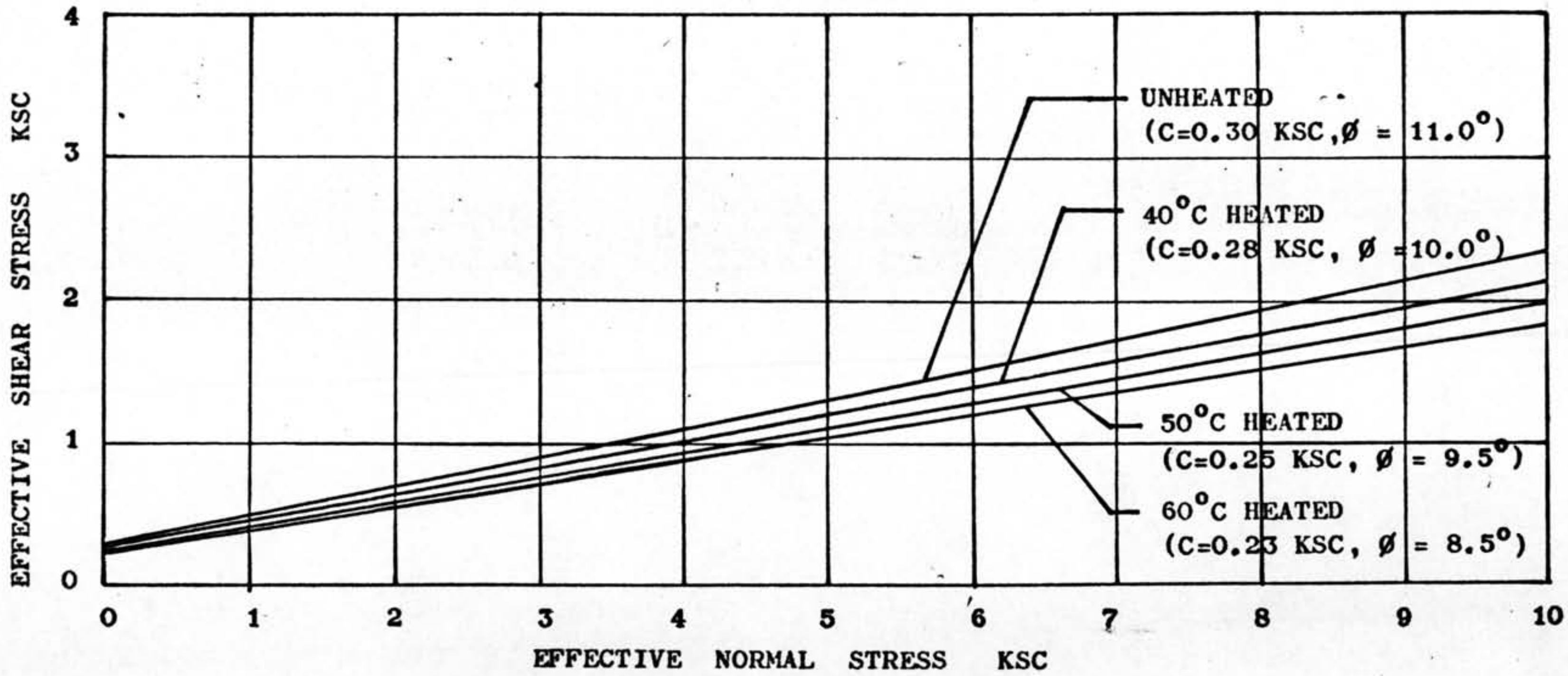

FIG. 13 COMPARISON OF TANGENT LINES OF MOHR'S CIRCLES, UNHEATED, HEATED AT 40°C, 50°C AND 60°C SAMPLES.
SAMPLE NO. B-2

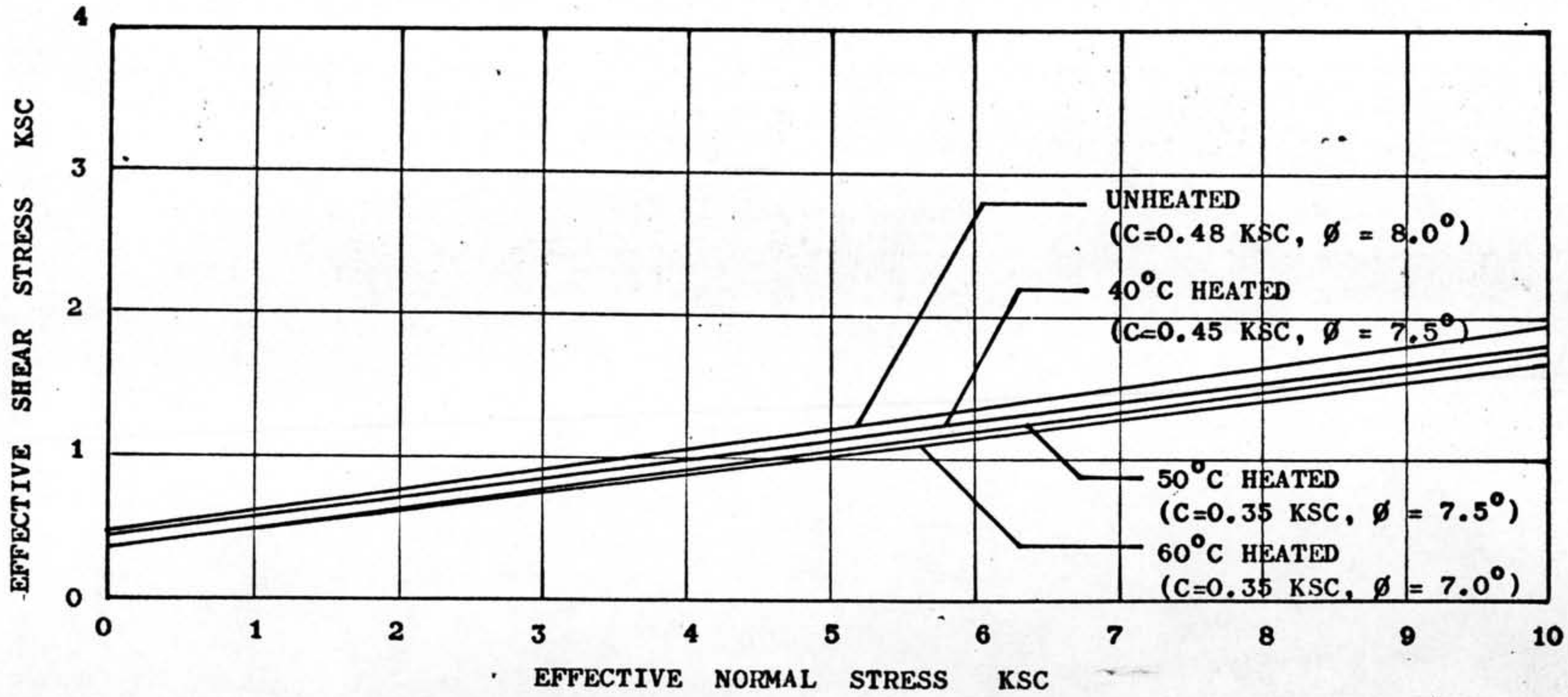

FIG. 14 COMPARISON OF TANGENT LINES OF MOHR'S CIRCLES, UNHEATED, HEATED AT 40°C, 50°C AND 60°C SAMPLES.
SAMPLE NO. B-3

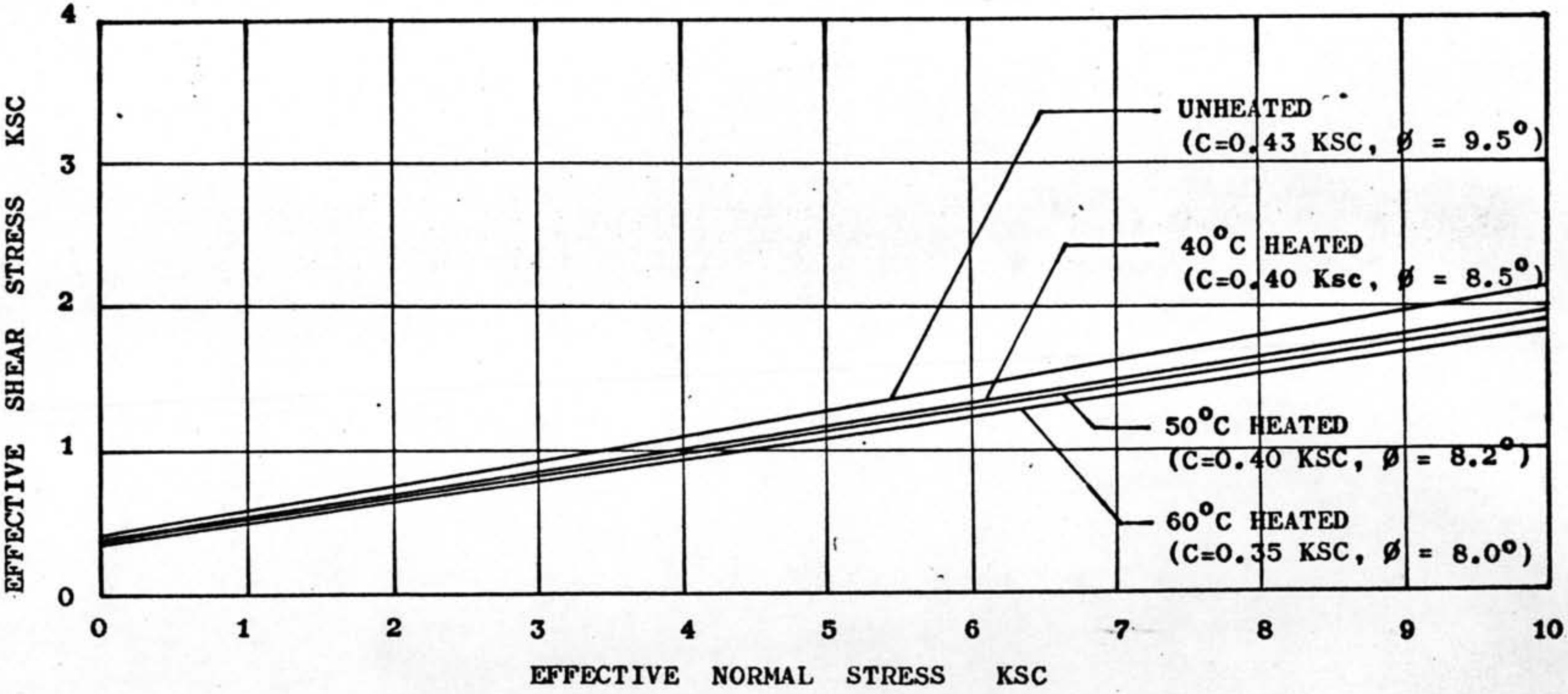

FIG. 15 COMPARISON OF TANGENT LINES OF MOHR'S CIRCLES, UNHEATED, HEATED AT 40°C, 50°C AND 60°C SAMPLES.
SAMPLE NO. B-4

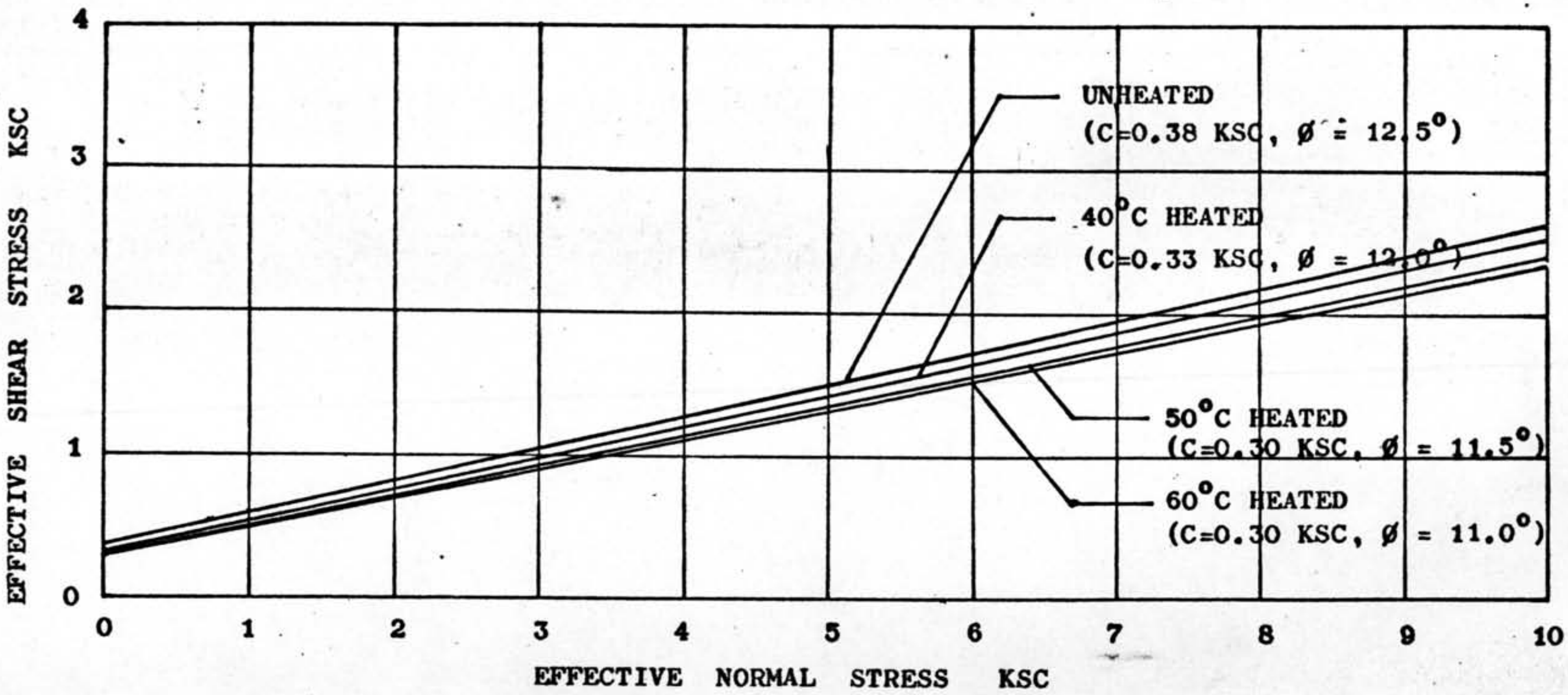

FIG. 16 COMPARISON OF TANGENT LINES OF MOHR'S CIRCLES, UNHEATED, HEATED AT 40°C, 50°C AND 60°C SAMPLES.
SAMPLE NO. B-5

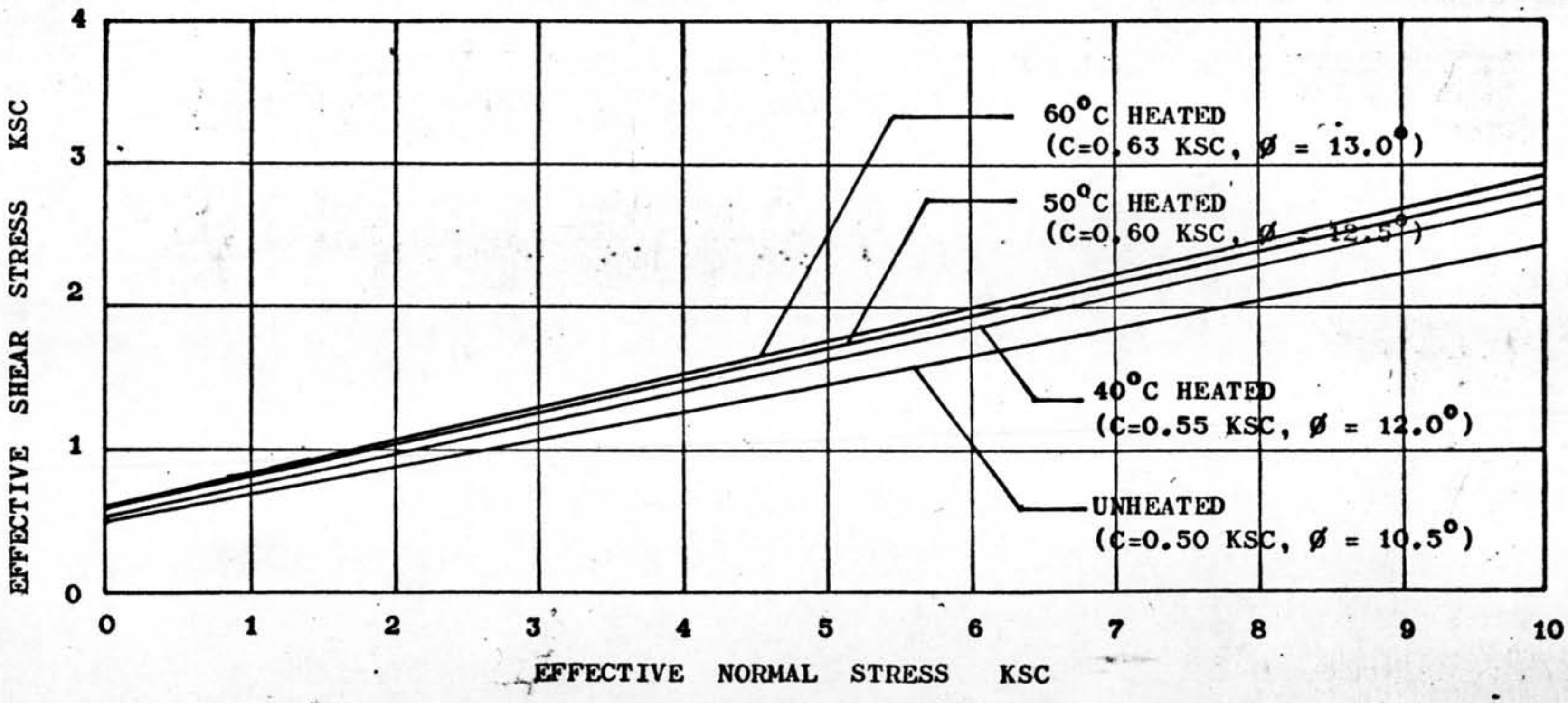

FIG. 17 COMPARISON OF TANGENT LINES OF MOHR'S CIRCLES, UNHEATED, HEATED AT 40°C, 50°C AND 60°C SAMPLES.

SAMPLE NO. B-6

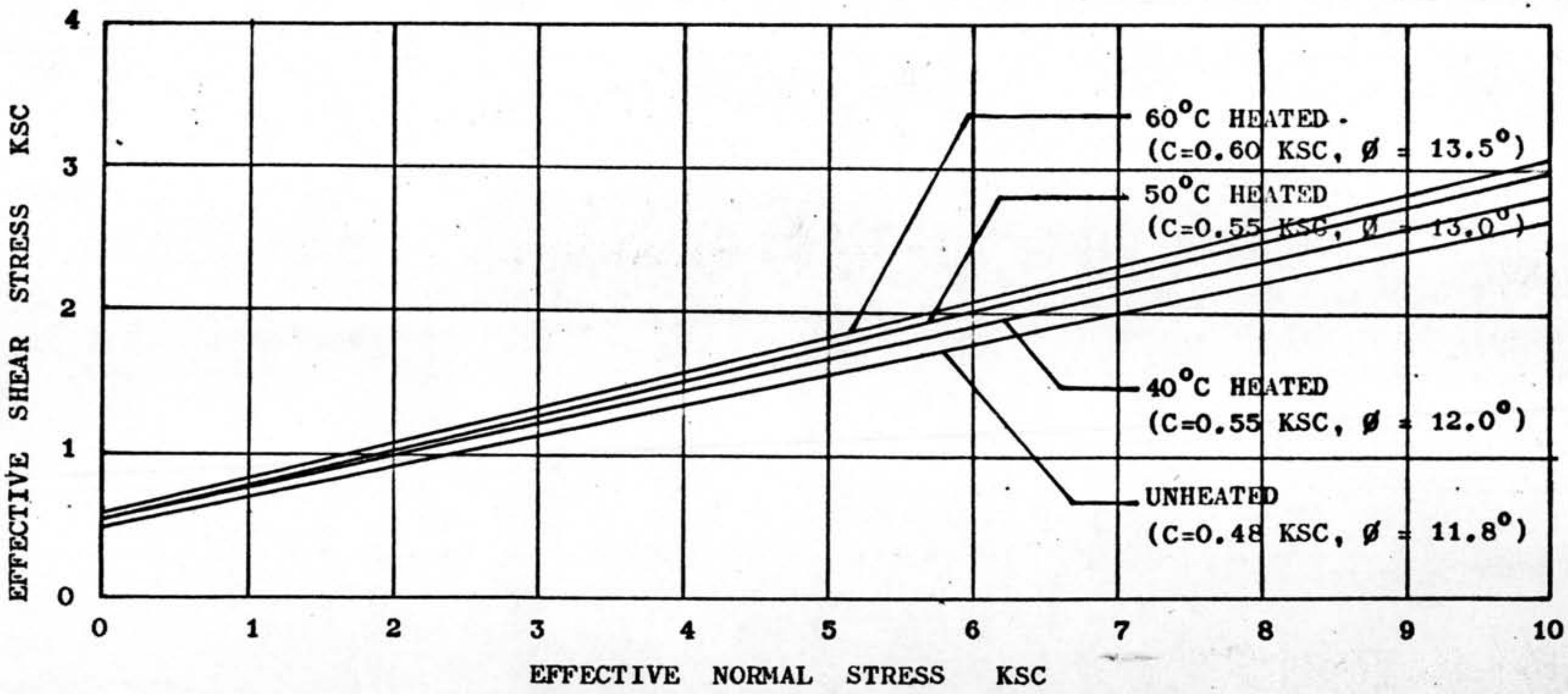

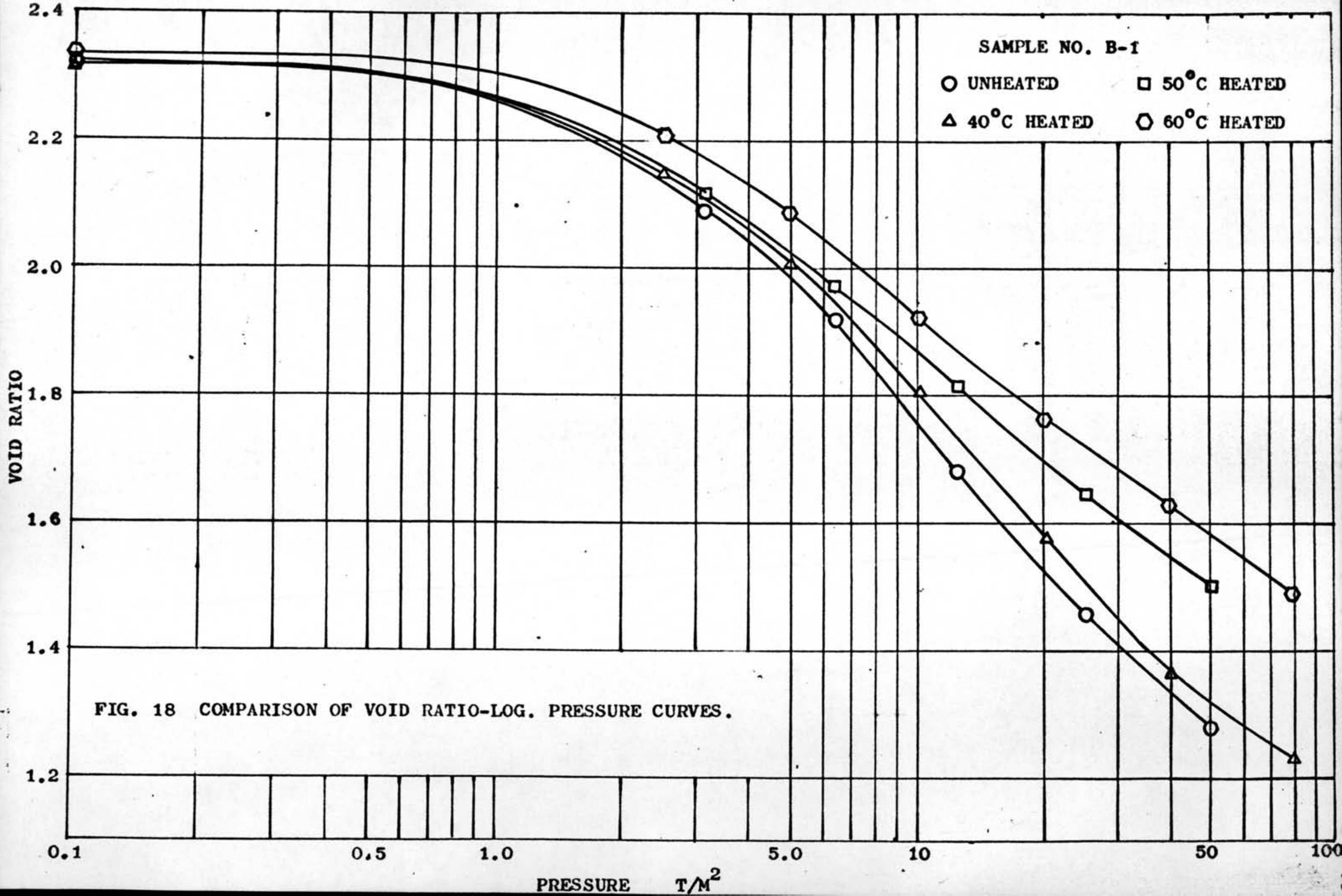

FIG. 18 COMPARISON OF VOID RATIO-LOG. PRESSURE CURVES.

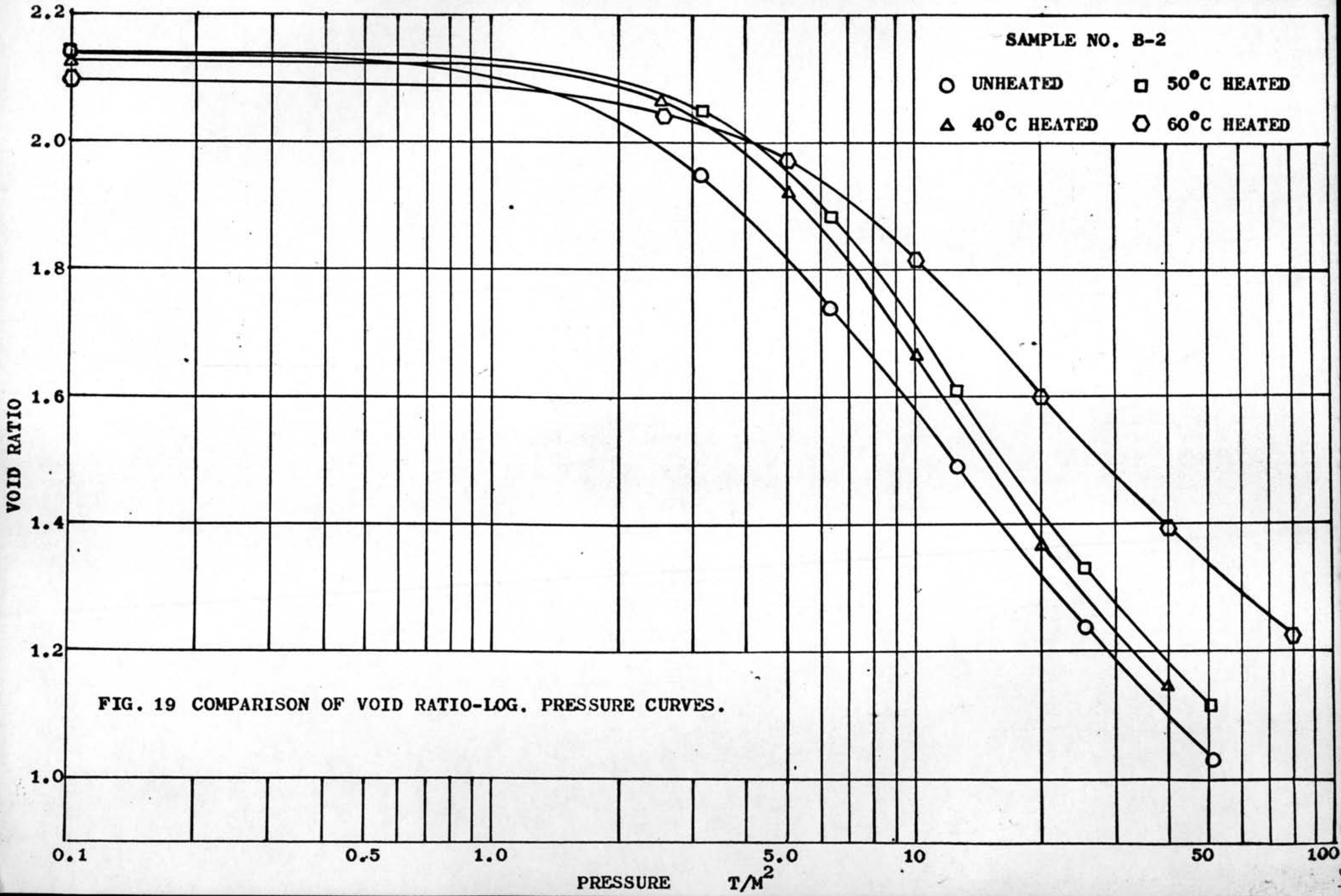

FIG. 19 COMPARISON OF VOID RATIO-LOG. PRESSURE CURVES.

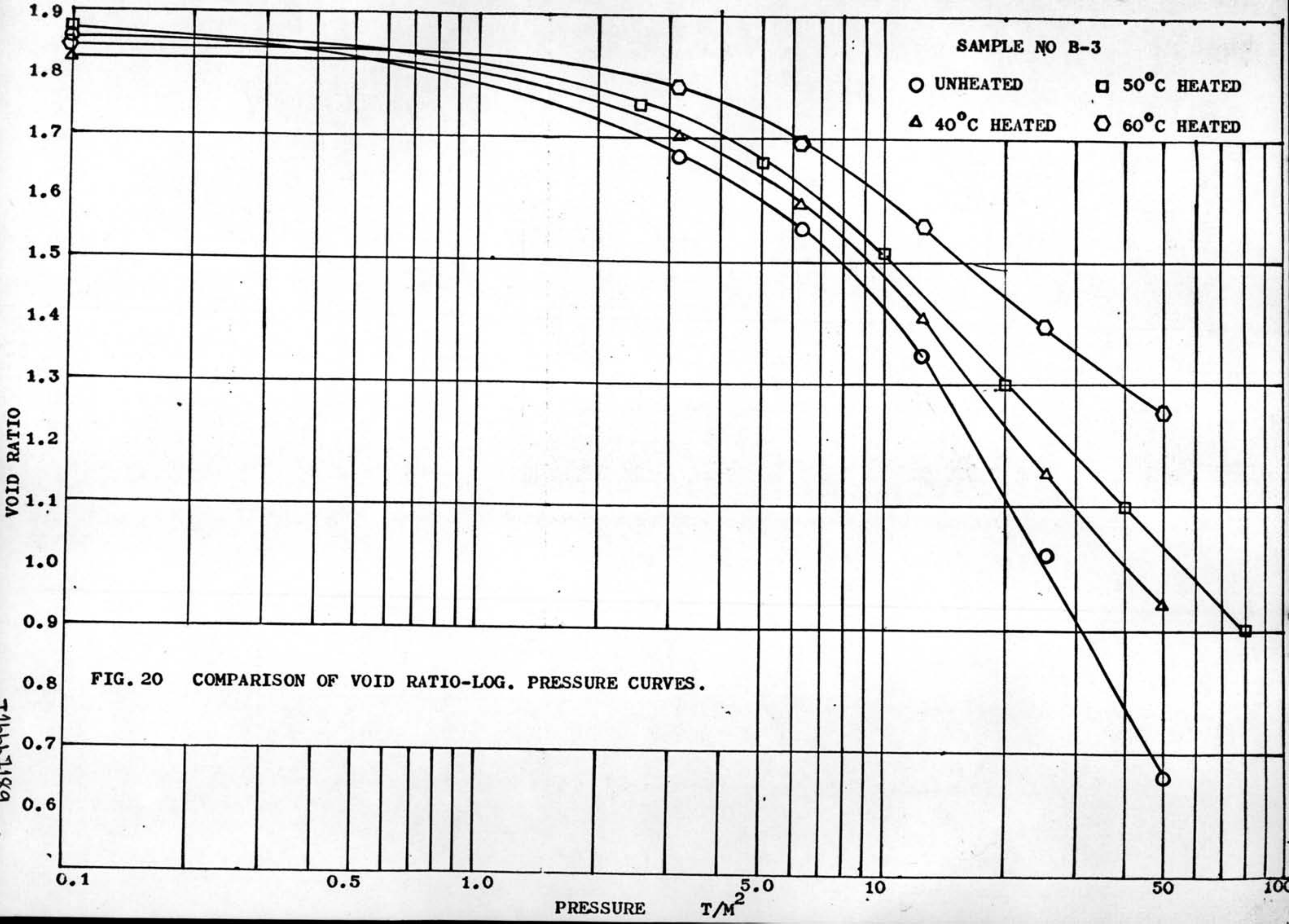

FIG. 20 COMPARISON OF VOID RATIO-LOG. PRESSURE CURVES.

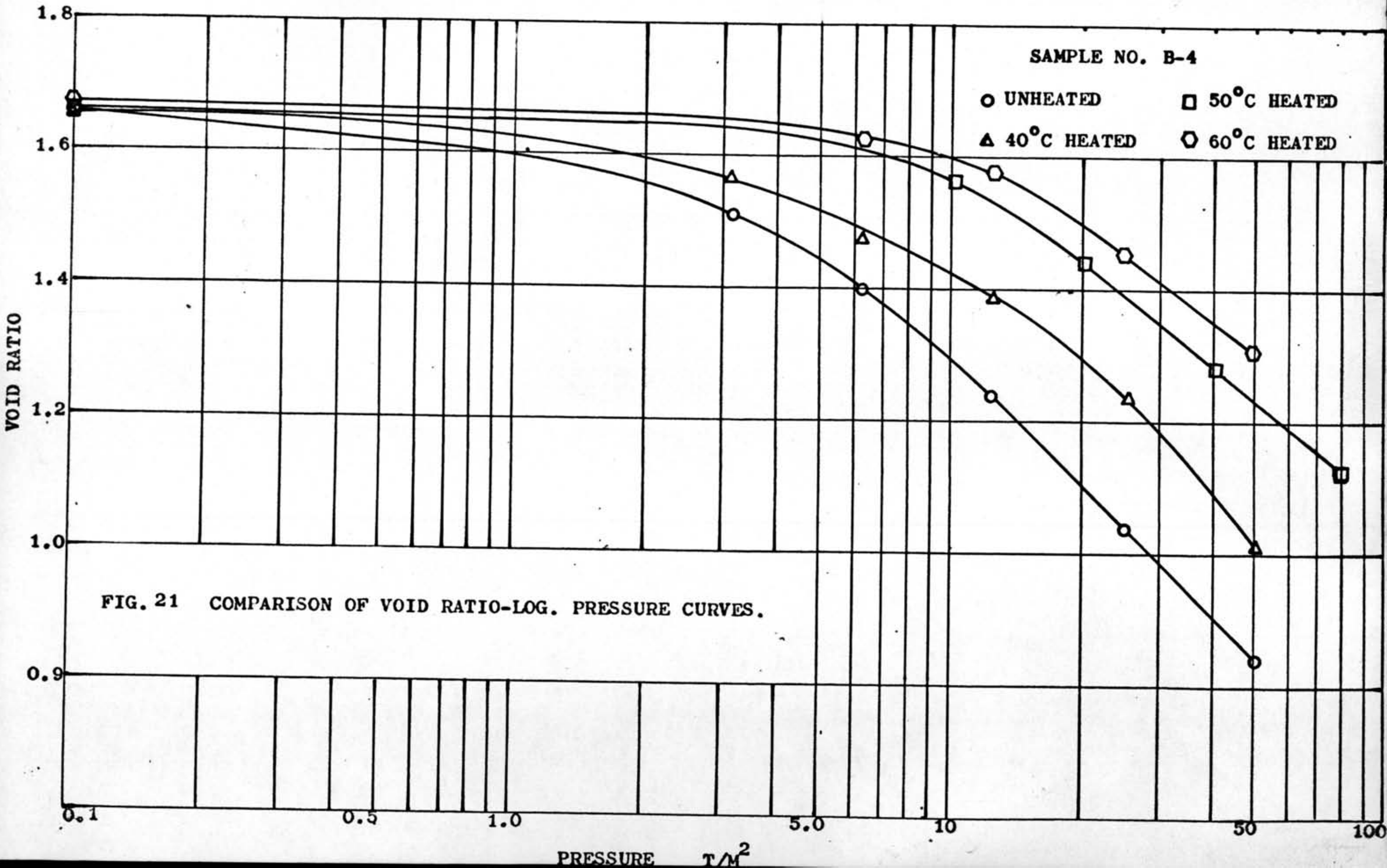

FIG. 21 COMPARISON OF VOID RATIO-LOG. PRESSURE CURVES.

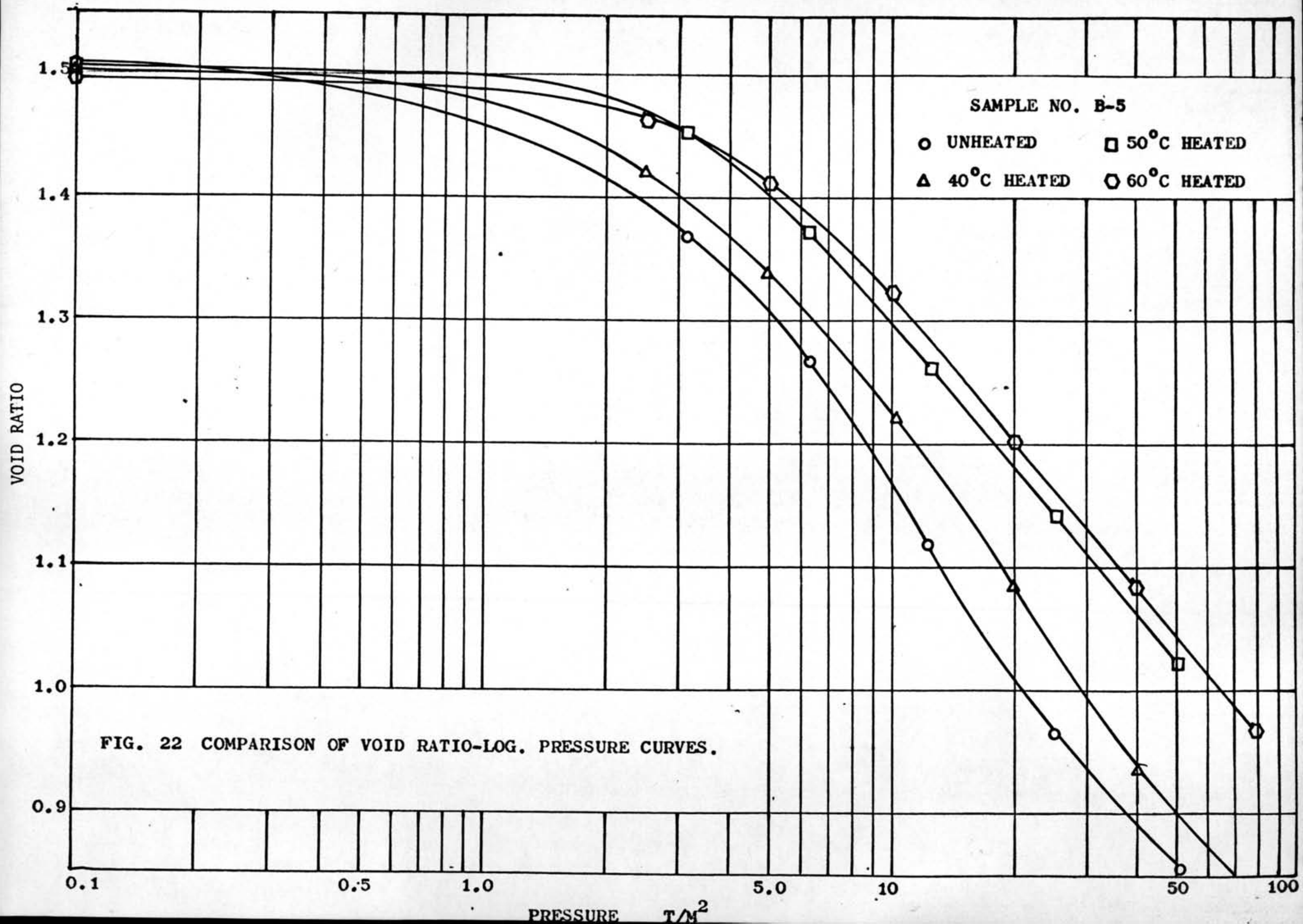

FIG. 22 COMPARISON OF VOID RATIO-LOG. PRESSURE CURVES.

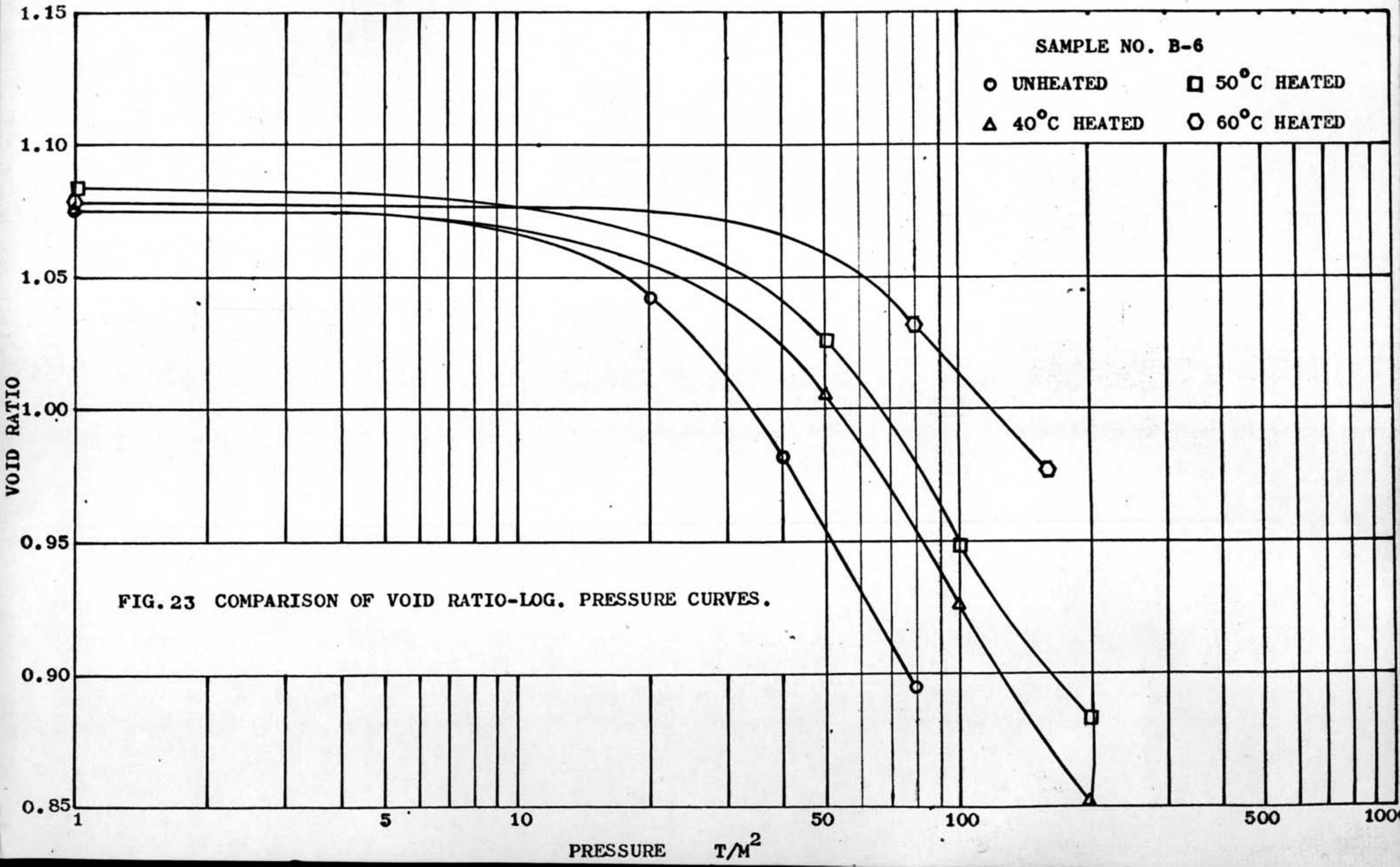

FIG. 23 COMPARISON OF VOID RATIO-LOG. PRESSURE CURVES.

FIG. 24 COMPARISON OF COEFFICIENT OF CONSOLIDATION C_v & PRESSURE CURVES,

SAMPLE B-1

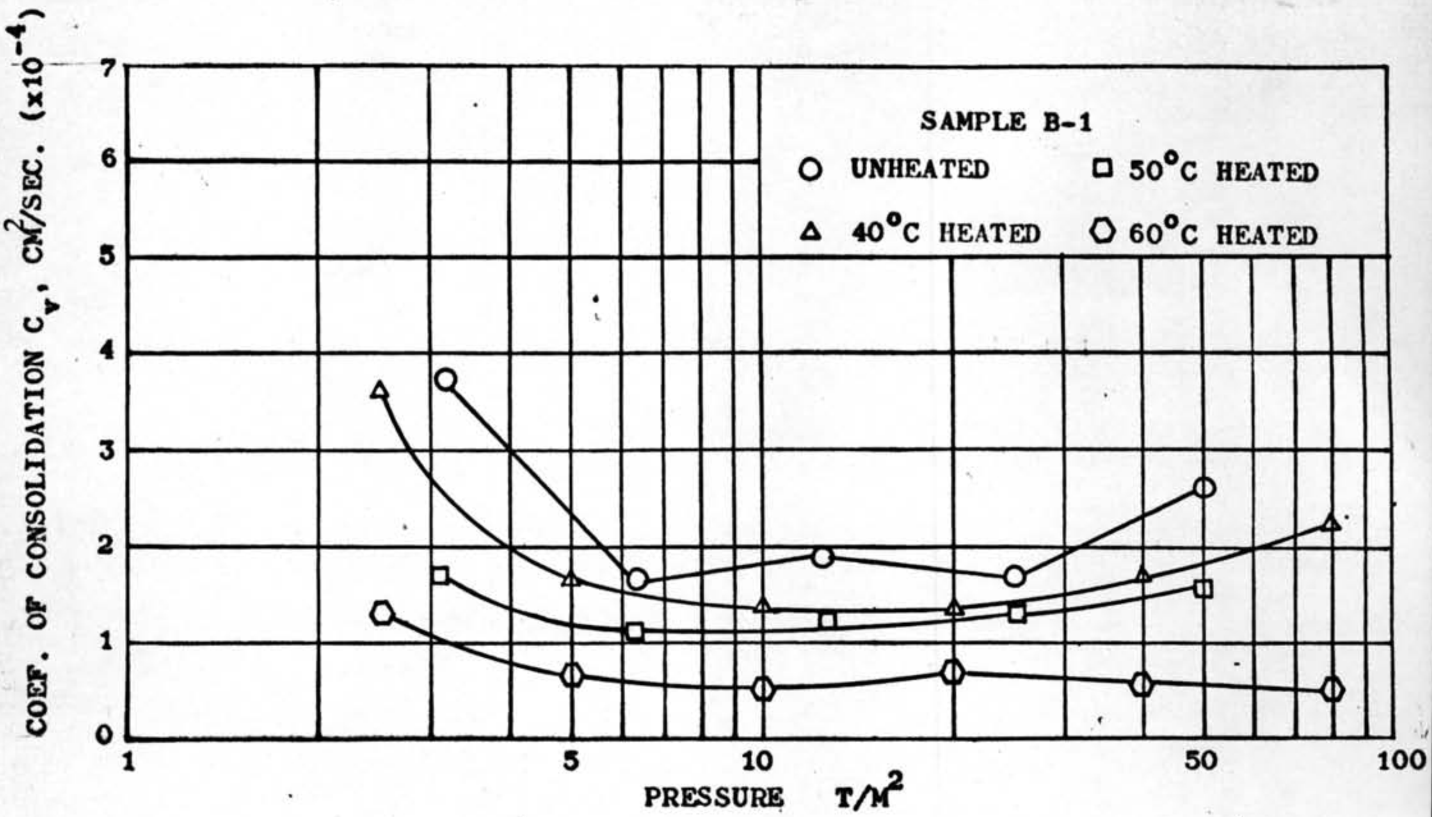

FIG. 25 COMPARISON OF COEFFICIENT OF CONSOLIDATION C_v & PRESSURE CURVES.

SAMPLE B-2

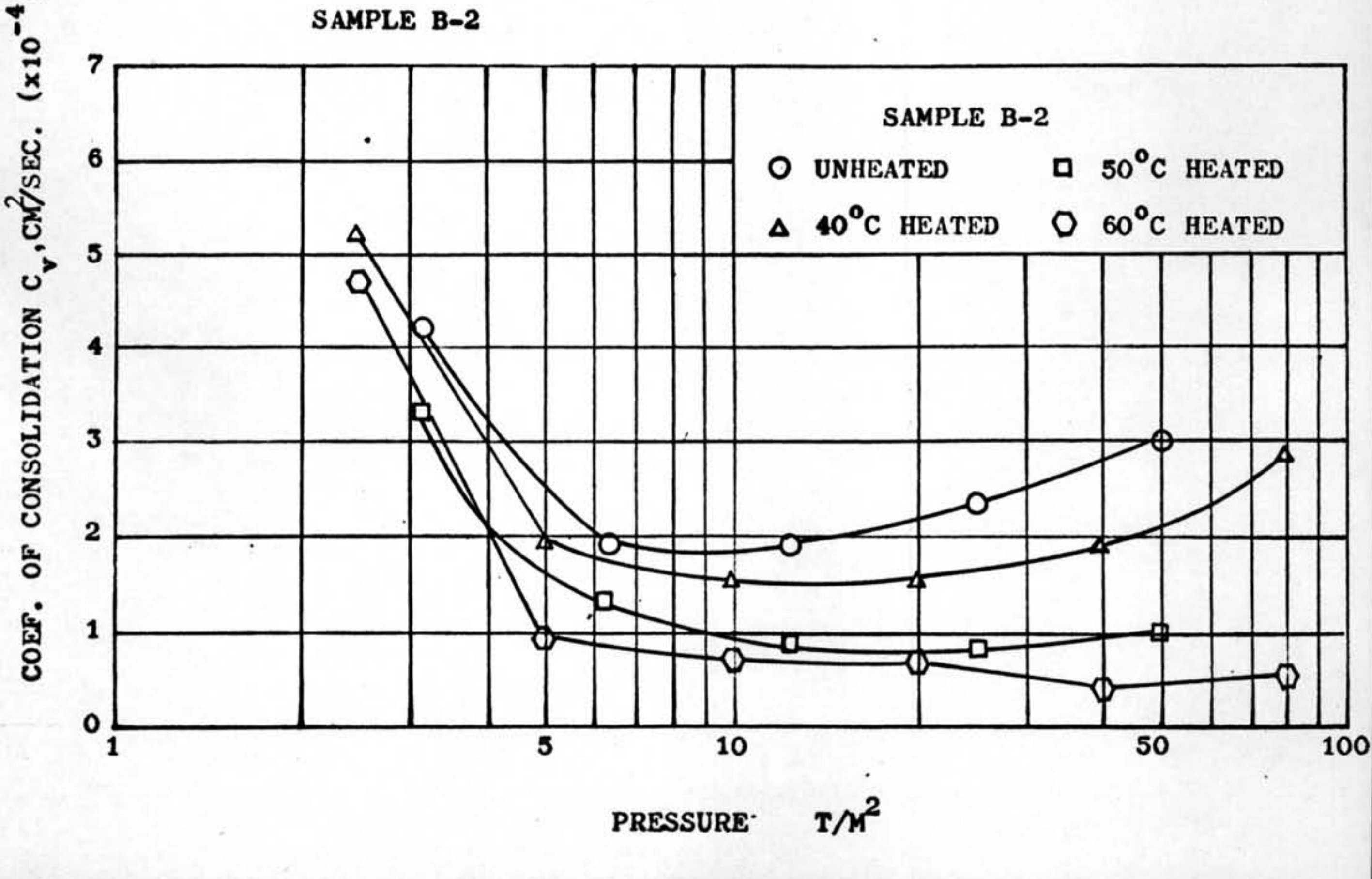

FIG. 26 COMPARISON OF COEFFICIENT OF CONSOLIDATION C_v & PRESSURE CURVES, SAMPLE B-3

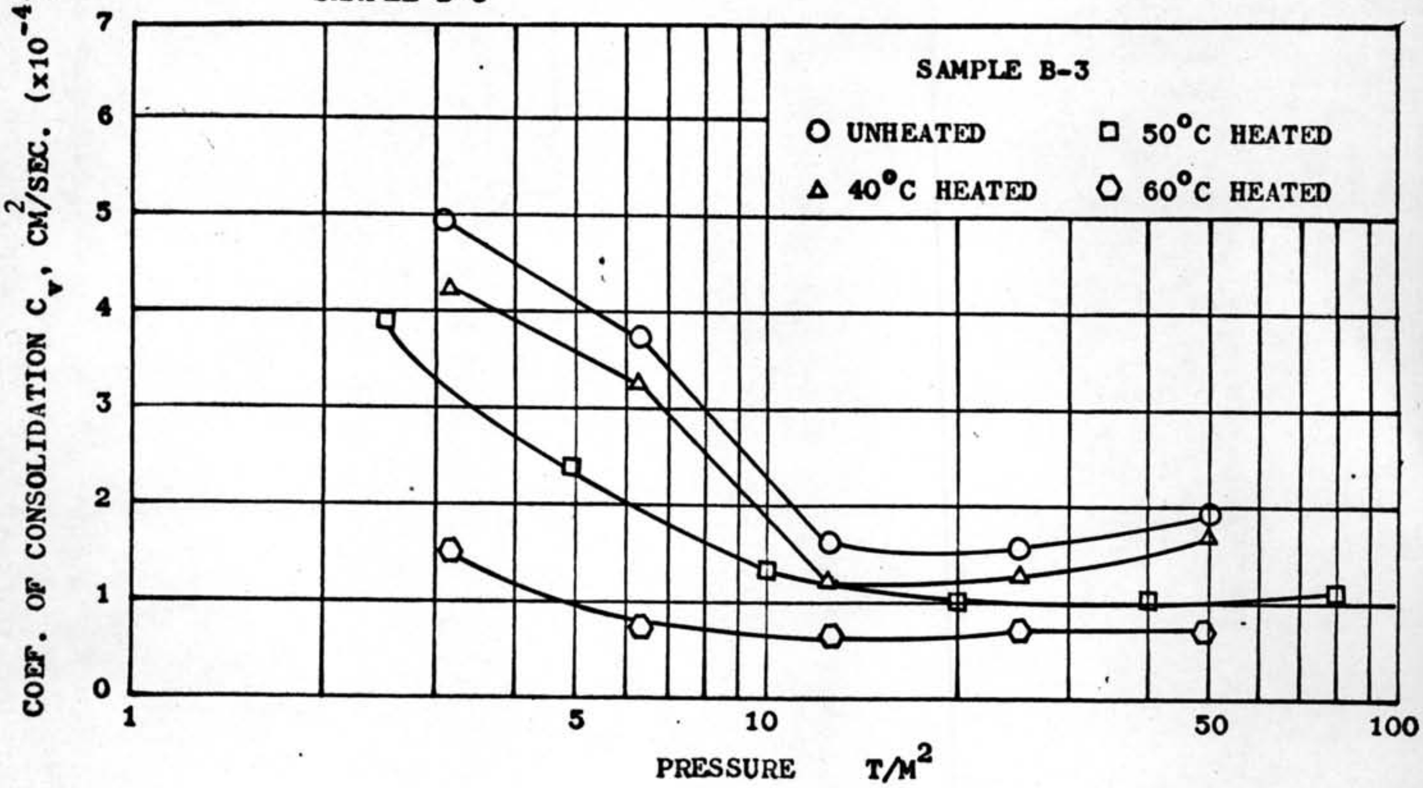

FIG. 27 COMPARISON OF COEFFICIENT OF CONSOLIDATION C_v & PRESSURE CURVES, SAMPLE B-4

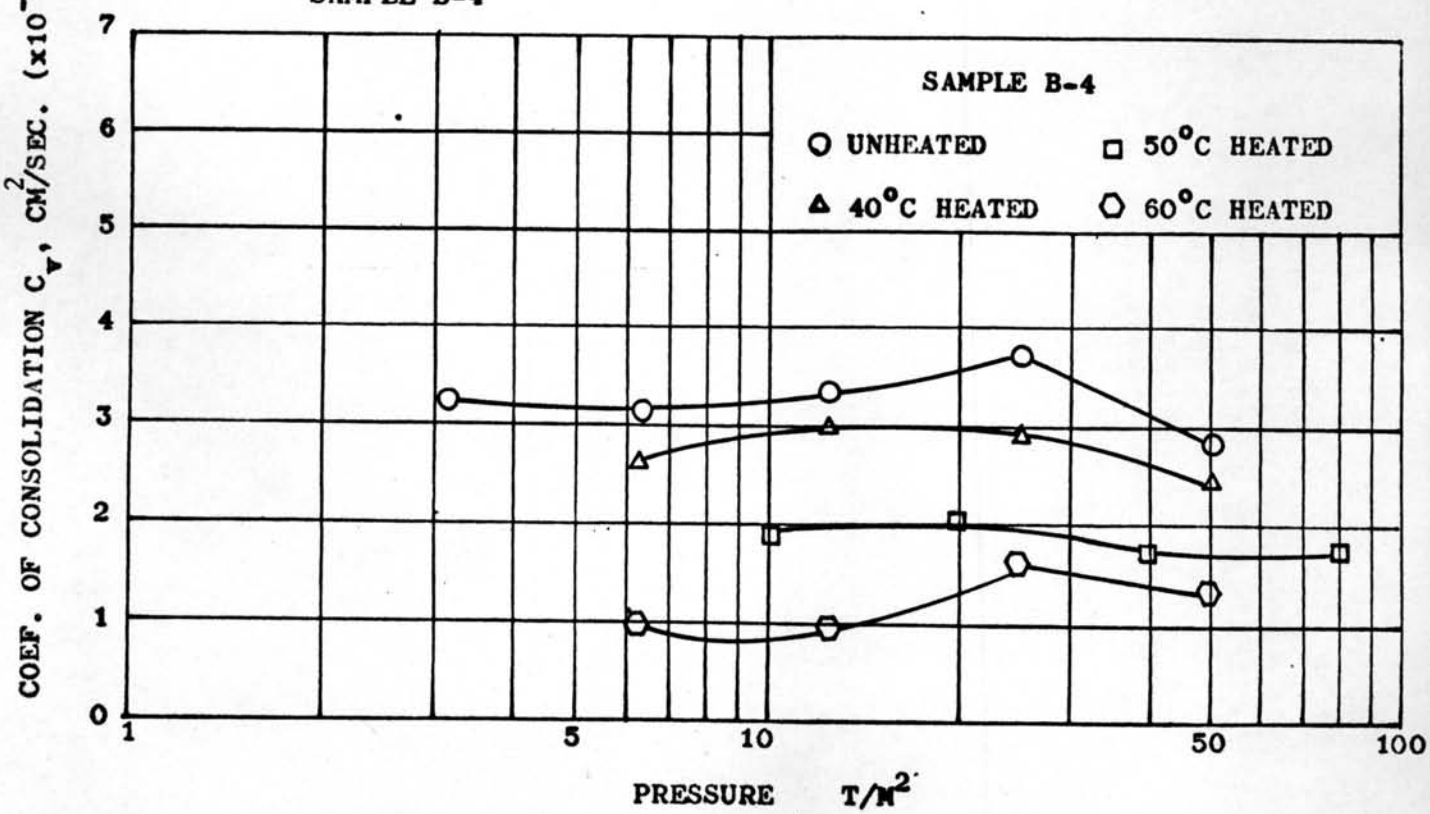

FIG. 28 COMPARISON OF COEFFICIENT OF CONSOLIDATION C_v & PRESSURE CURVES, SAMPLE B-5

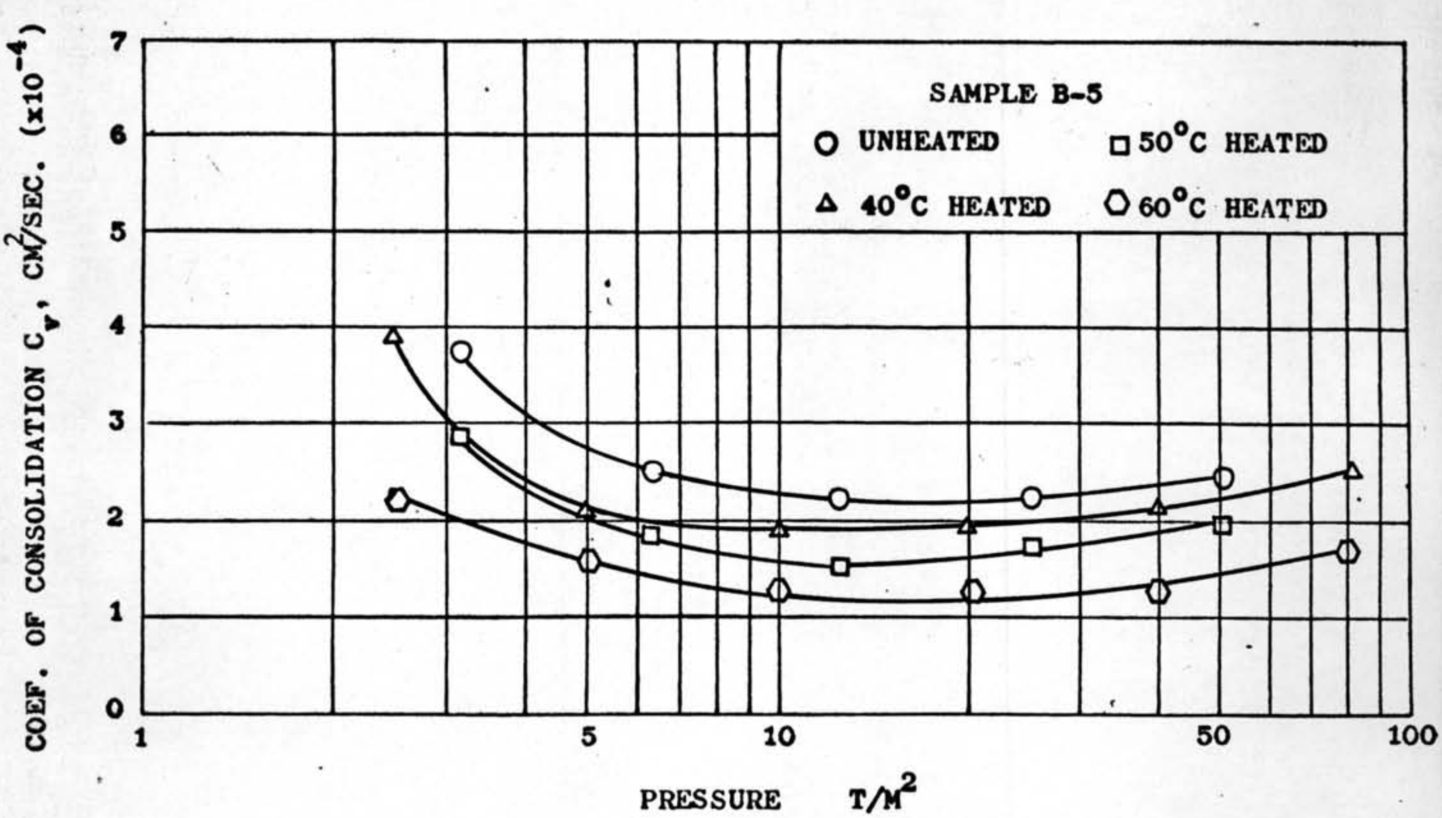

FIG. 29 COMPARISON OF COEFFICIENT OF CONSOLIDATION C_v & PRESSURE CURVES, SAMPLE B-6